2.9 MULTIASTRAL 3-CONFIGURATIONS

A geometric configuration is said to be of **symmetry type** $[h_1, h_2]$ provided its points form h_1 orbits, and its lines h_2 orbits under the group of its isometric symmetries. We shall also say that such a configuration is $[h_1, h_2]$**-astral**, or, if the precise values of h_1 and h_2 are not important in the discussion, that it is **multiastral**. Clearly, if a configuration of type [q, k] is $[h_1, h_2]$-astral then $h_1 \geq (k+1)/2$ and $h_2 \geq (q+1)/2$. If h_1 and h_2 have these minimal values we shall simplify the language and say that the configuration is **astral**. In cases where $h_1 = h_2 = h$, we shall say that the configuration is h**-astral.**

The study of these configurations is much less advanced, and promises to be more challenging than the investigation of the 2-astral 3-configurations. There are two sources of the variety possible for h-astral 3-configurations. On the one hand, similarly to the situation with dihedral astral configurations, in many cases there is at least one parameter that can assume a continuum of different real values. On the other hand, if $h \geq 3$, a line of the configuration can contain points from either two or three different orbits. The case $h = 2$ is radically different from those with $h \geq 3$.

The h-astral 3-configurations come in three varieties:

- **projectively h-astral**, that is, configurations that are h-astral in the *extended Euclidean* (that is, *projective*) plane E^{2+}, but not in the Euclidean plane E^2 itself.
- **h-chiral** that is, configurations in the Euclidean plane E^2, with a cyclic symmetry group.
- **h-dihedral,** that is configurations in the Euclidean plane E^2, with a dihedral symmetry group.

Throughout, the use of a numerical prefix h- means that there are *at most* h orbits of points and *at most* h orbits of lines, with *equality in at least one case*.

Examples of **projectively astral** configurations are shown in Figure 2.9.1 and 2.9.2. The configuration in Figure 2.9.1 is a realization of the Pappus configuration. Two 3-astral realization of the Desargues configuration (10_3) in E^{2+} are shown in Figure

2.9.2; they are among the illustrations given by Coxeter [C8]. Two examples of projectively 3-astral configurations (15_3) are shown in Figure 2.9.3. It is clear that similar examples of projectively h-astral configurations could be found for all $h \geq 4$. At least for small h, the complete characterization of projectively astral configurations may be feasible but has not been worked out.

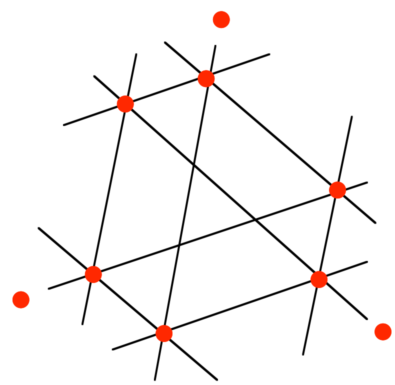

Figure 1. A 3-astral version of the Pappus configuration (9_3) in the extended Euclidean plane.

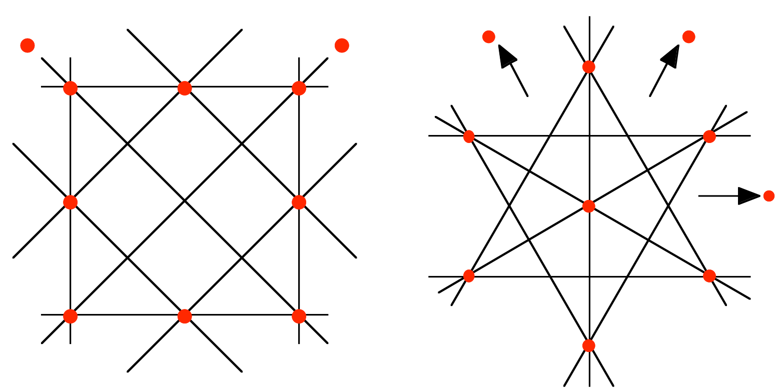

(a) (b)

Figure 2.9.2. Two projectively 3-astral realizations of the Desargues configuration (10_3) (after [C8]). In (b) the line at infinity is included.

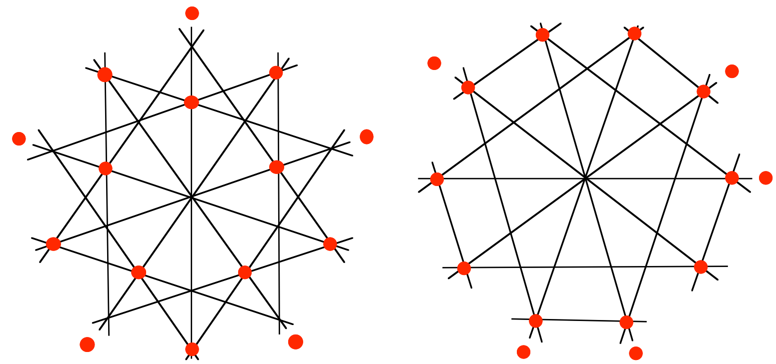

Figure 2.9.3. Two examples of projectively 3-astral configurations (15_3). Notice that the one at left is [3, 2]-astral, and the one at right is [2, 3]-astral.

h-chiral astral configurations (n_3) are much more interesting. We have discussed the 2-astral chiral configurations in Section 2.7. For $h \geq 3$ there is more than one possibility. We begin by explaining the notation for h-chiral configurations in which each line is incident with points of two orbits only; the remaining case — some lines incident with three orbits of points — will be described later. The notation used in Section 2.7 will be expanded here; the general form for h-chiral configurations (n_3) of this kind is $m\#(b_1, b_2, \dots, b_h; b_0; \lambda_1, \lambda_2, \dots, \lambda_{h-2})$ — or in a shorter symbol $m\#(b_1, b_2, \dots, b_h; b_0)$. Here $n = hm$ and we have $h–2$ real parameters λ_j besides $h+1$ discrete ones b_j. Together these parameters lead to a quadratic equation for an additional parameter λ. This equation can have 2, 1 or 0 real solutions — in the last case there are no corresponding real configurations. Our explanation is illustrated in Figure 2.9.4, using a 3-chiral configuration (27_3) as an example.

The detailed study of h-chiral configurations was initiated by Boben and Pisanski [B20] under the name "polycyclic configurations", and with slightly different notation. As pointed out in [B20], the dual of a configuration $m\#(b_1, b_2, \dots, b_h; b_0)$ is the configuration $m\#(b_h, b_{h-1}, \dots, b_1; b_1+b_2+ \dots +b_h–b_0)$. For $h = 2$ this reduces to the facts we shall discuss at length in Section 2.10.

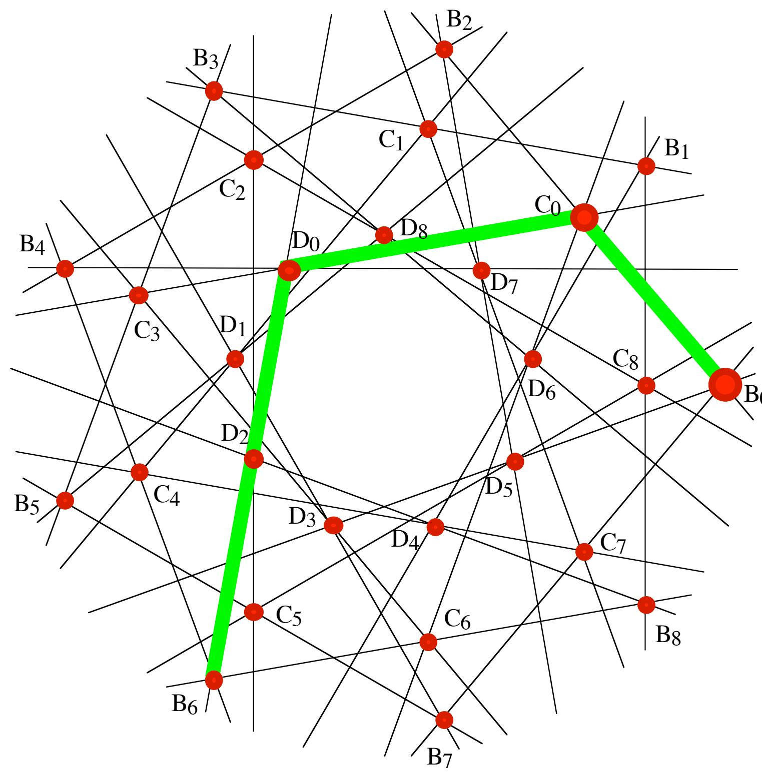

Figure 2.9.4. The characteristic path in a 3-chiral configuration (27_3).

As mentioned earlier, the symbol for an h-chiral configuration (n_3), where $n = hm$, is of the form $m\#(b_1, b_2, \ldots, b_h; b_0; \lambda_1, \lambda_2, \ldots, \lambda_{h-2})$; the parameters are again determined along a **characteristic path**. The entries $b_1, \ldots, b_h$ are the spans of the diagonals in the different regular m-gons that are determined by the path; all the diagonals are oriented in the same way — all clockwise or all counterclockwise — and the real numbers $\lambda_1, \lambda_2, \ldots, \lambda_{h-2}$ denote the ratios in which each diagonal determined by a segment of the path is divided by the endpoint of the segment. The path returns to the starting polygon, but not necessarily to the starting point of the path. The parameter b_0 indicates the vertex of the starting polygon at which the characteristic path ends. These data lead to a quadratic equation for the ratio λ on the next-to-last segment; the ratio applicable to the last segment is then completely determined. Thus there are either two, or one, or no real geometric configurations corresponding to a given symbol. There are also possibilities of unintended incidences similar to the ones we encountered earlier, hence we are in general talking about **representations** of the symbols, rather than **realizations**. In case the parameters $\lambda_1, \lambda_2, \dots, \lambda_{h-2}$ in a symbol m#($b_1, b_2, \dots, b_h; b_0; \lambda_1, \lambda_2, \dots, \lambda_{h-2}$) are not relevant or not known, we abbreviate the symbol to m#($b_1, b_2, \dots, b_h; b_0$).

The example in Figure 2.9.4 presents a 3-chiral configuration with symbol 9#(2,3,2;6;0.5). The points of the three orbits are denoted by B_j, C_j, D_j. The determination of the symbol is highlighted by the three-step characteristic path. Note that the ratio λ_1 can be chosen freely, and in the illustration it was taken as $\lambda_1 = 0.5 = C_0B_0/B_2B_0$. Once the first h-2 ratios λ_j are chosen, the last ratio λ_{h-1} (determining the position of the point of last orbit on the penultimate diagonal) is determined by a quadratic equation. (For details see [B20].) In the illustration we have $h = 3$, hence $\lambda_{h-1} = \lambda_2$ (which is about 2/3). Naturally, the symbol is not unique since it depends, besides the λ_j's for $h \geq 3$, on the orbit of the starting point, and on the orientation chosen. The influence of the parameter λ_{h-2} is illustrated in Figure 2.9.5.

Using symbols like u, v, w, ... for elements of the different orbits of points, we can say that the h-chiral configurations considered so far have lines of type {u,u,v}, {v,v,w}, ... But other possibilities exist in which the incidences of lines with orbits of the points are different. For example, in case h = 3, it is possible to have three orbits of lines, all three of the type {u,v,w}, or else, one of the type {u,v,w} and the other two of types {u,v,v} and {u,w,w}. Three example of the former variety are shown in Figure 2.9.6, while examples of the second kind are illustrated in Figure 2.9.7; the diagrams in Figure 2.2.1 show the $(9_3)_2$ and $(9_3)_3$ configurations, which is of these two kinds. A notation for the configurations in Figure 2.9.6 is explained in the caption. An apparently convenient notation is proposed for the kind of configurations shown in Figure 2.9.7. It assigns the first symbol to the line and the point that are incident with three orbits of the other kind, and the other symbols in the obvious manner. For the notation one conveniently chooses the one that involves the smallest maximal parameter. No additional details about either of these kinds of configurations are available as of this writing.

Naturally, for $h \geq 4$ it is possible to imagine an increasingly large number of types of h-chiral configurations. However, so far nothing has been done in this direction.

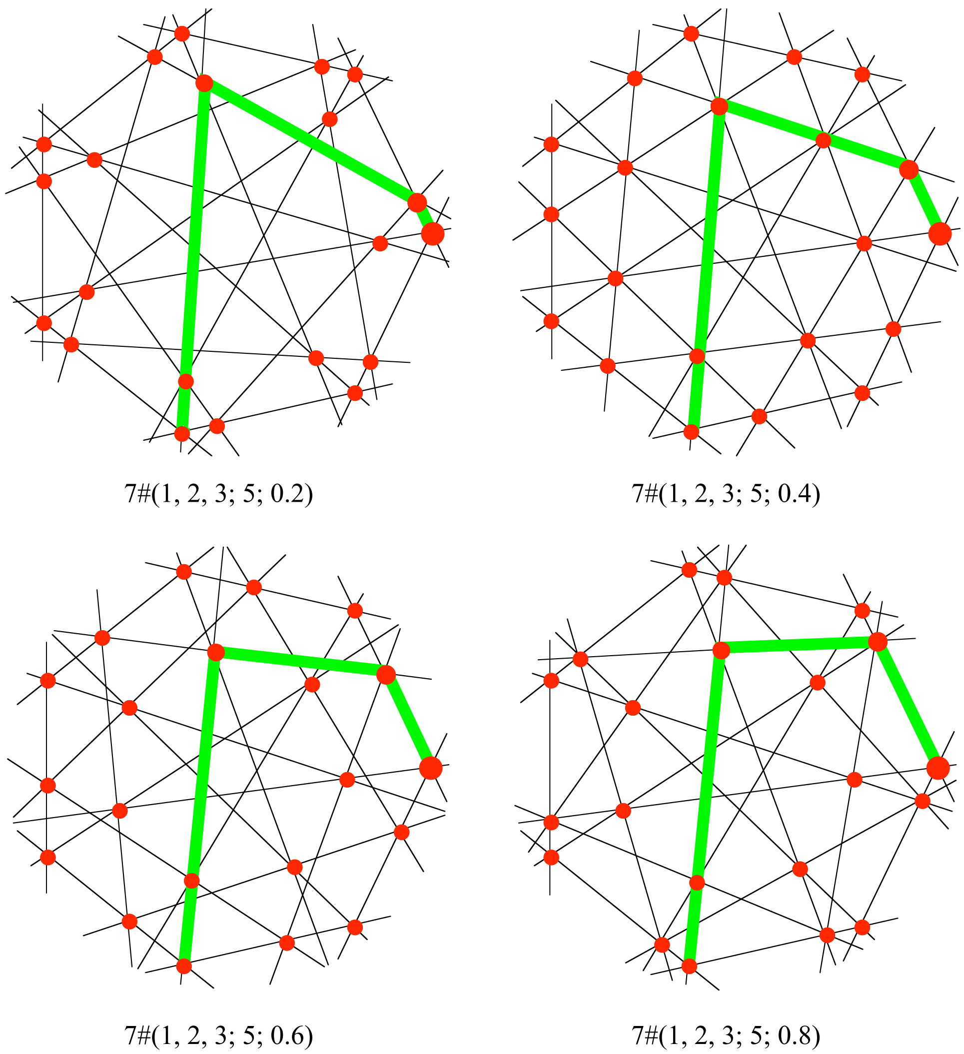

Figure 2.9.5. An illustration of the dependence of a 3-chiral configuration (21_3) on the parameter λ_1.

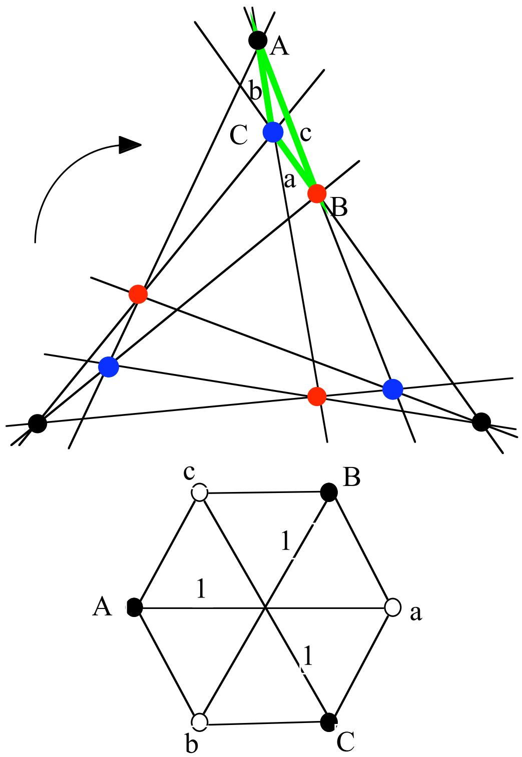

(a) 3#[1,1,1;0]

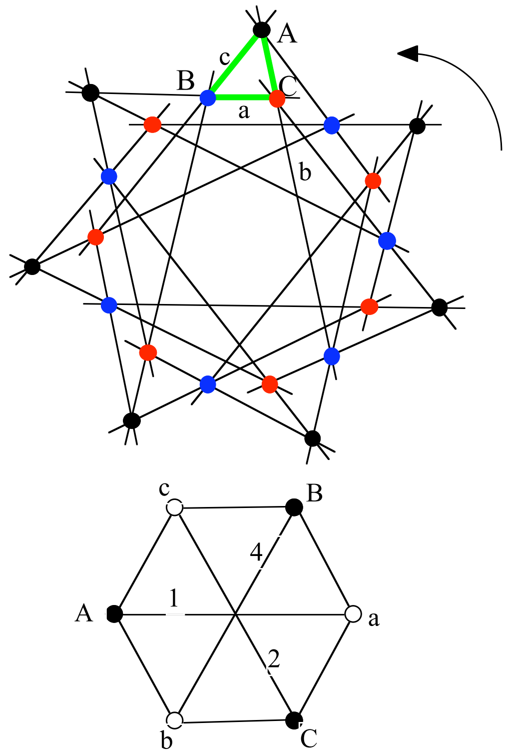

(b) 7#[1,4,2;0]

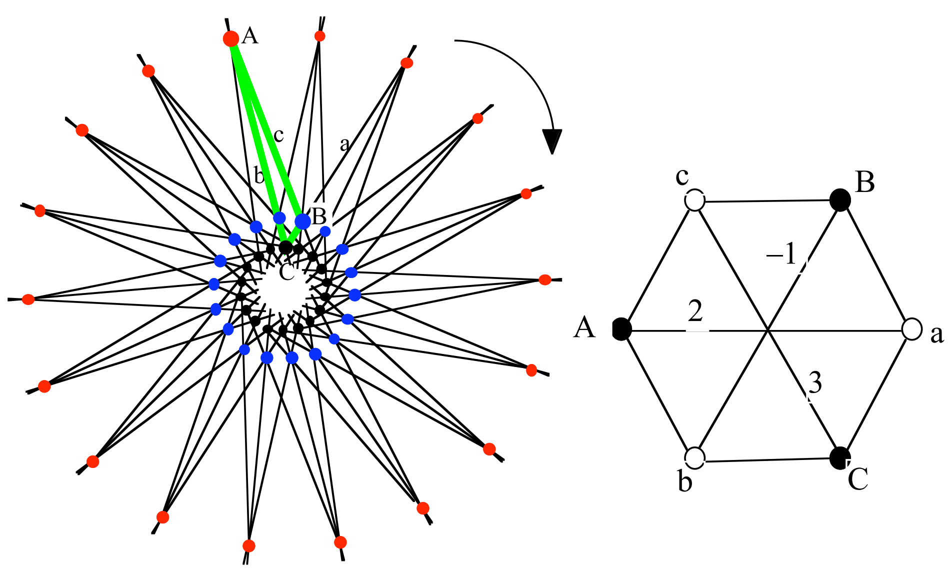

(c) 18#[2,-1,3;0]

Figure 2.9.6. Two examples of 3-chiral configurations in which every line meets all three orbits of points, and every point meets lines of the three orbits. The characteristic path (which does not have to be closed) leads to a symbol for the configuration. The configuration in (a) is another realization of the Pappus configuration. With each we show a reduced Levi diagram.

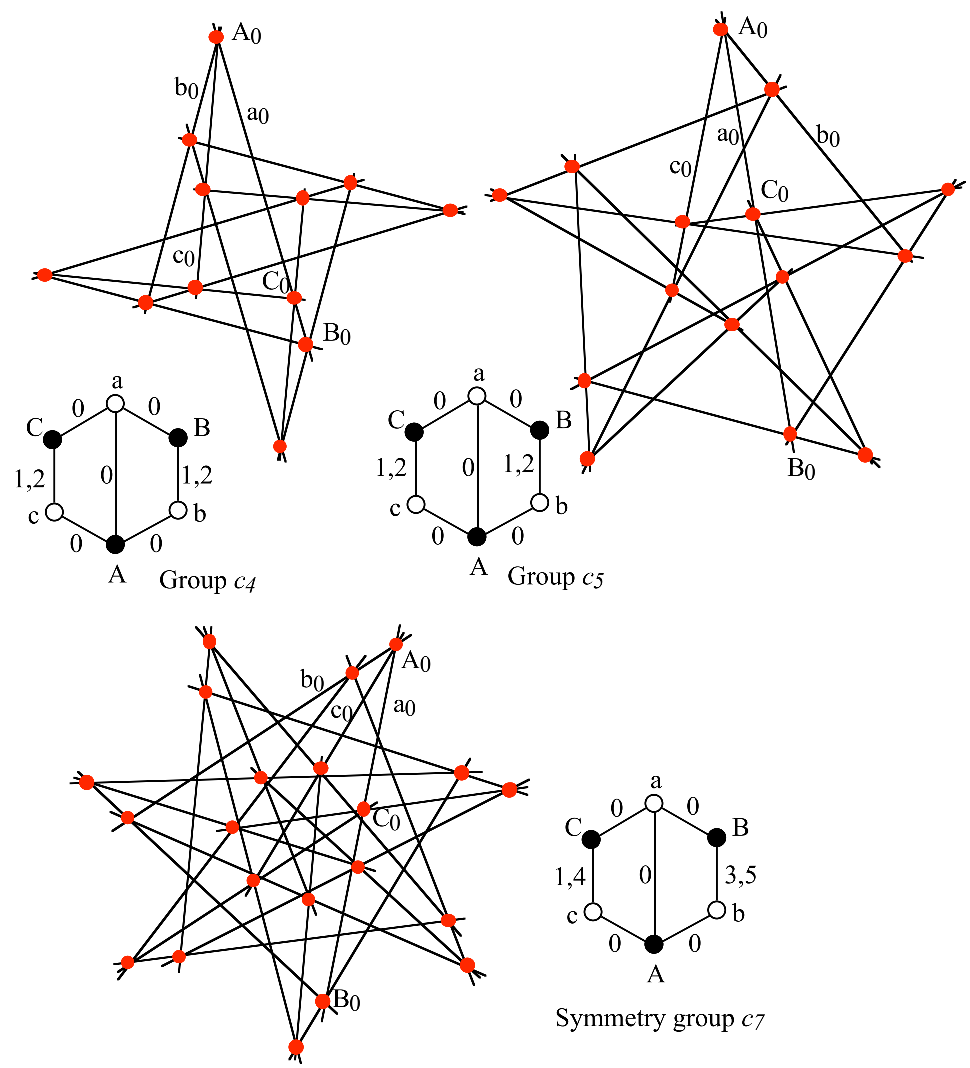

Figure 2.9.7. Examples of 3-chiral configurations in which each line of one orbit is incident with points of each of three orbits, while the other lines are incident with two points from one orbit and one point from another orbit. Each is accompanied by a reduced Levi diagram. As symbols for these configurations we can use 4#[1,2;1,2], 5#[1,2;1,2] and 7#[1,4;3,5]. The configuration 5#[1,2;1,2] appears in van de Craats [V1].

h-dihedral configurations are unexplored as well. In Figures 2.9.8, 2.9.9 and 2.9.10 are shown a few examples. The examples in Figure 2.9.8 are obviously typical of an infinite class of analogous constructions. In Figure 2.9.9 only two orbits of points are shown, the points of the third orbit can be chosen at several distinct locations. This kind of configurations can obviously be generalized in a variety of ways. Figure 2.9.10 illustrates the degree of complication possible with h-astral configurations for larger h.

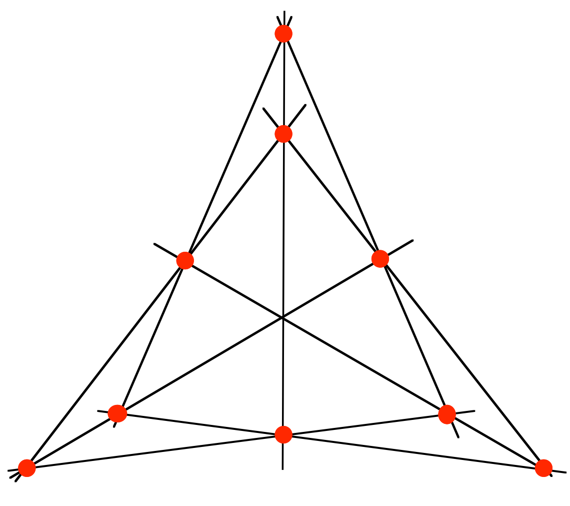

Figure 2.9.8. Two examples of 3-dihedral 3-configurations. The one at left is another realization of the Pappus configuration.

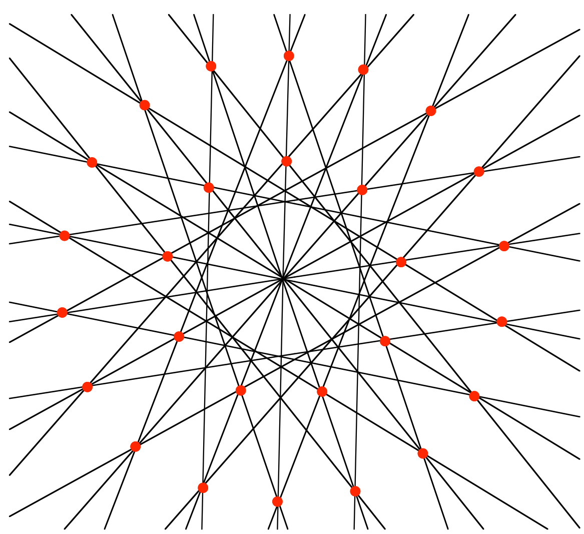

Figure 2.9.9. Adding an orbit of points at suitable intersections leads to several different 3–dihedral configurations. Notice that such configurations are, in fact, [3, 2]-dihedral.

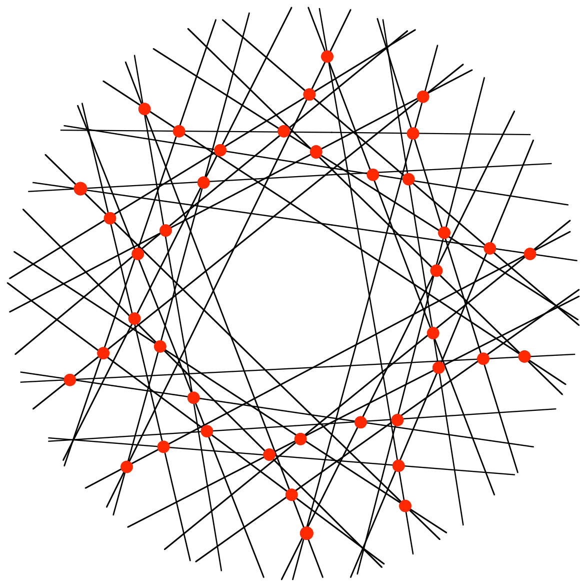

Figure 2.9.10. A [4,5]-dihedral configuration (40_3) found by L. Berman.

Exercises and problems 2.9

1. Decide whether the two configurations in Figure 2.9.3 are dual — or even polar –– to each other. Is either of them isomorphic to the (15_3) configuration in Figure 1.1.1?

2. Determine the number of distinct ways in which it is possible to replace the points in Figure 2.9.9 in such a way that the result is a [3, 2]-dihedral configuration.

3. By moving the outer vertices in Figure 2.9.8 along the mirror, a continuum of (projectively) distinct configurations can be obtained; all these are isomorphic. Are there any analogous configurations (15_3) that are not isomorphic to the one in Figure 2.9.8 ?

4. For $h_1 = 2$ and $h_1 = 3$, determine the possible values of h_2 for which there exist $[h_1, h_2]$-astral configurations of the various kinds. Provide examples for all existing types.

5. Construct examples of 4-chiral configurations (n_3) with the smallest n. Justify your answer. Generalize.

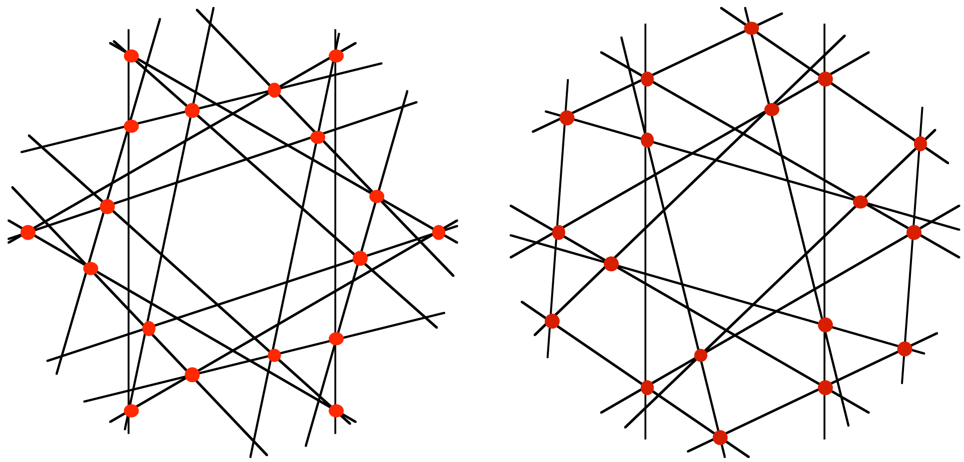

Figure 2.9.11. Two (18_3) 3-chiral configurations.

6. Determine the symbols of the two configurations is Figure 2.9.11.

7. Verify that the Cremona-Richmond configuration (15_3) shown in Figure 1.1.1 is of the type represented by the examples in Figure 2.9.7. Find its symbol.

8. Find the criteria for the property of the first two configurations of Figure 2.9.7 (but not the third) that there are only two orbits of points (and two orbits of lines) under automorphisms.